PCCP

Accepted Manuscript

This is an *Accepted Manuscript*, which has been through the Royal Society of Chemistry peer review process and has been accepted for publication.

Accepted Manuscripts are published online shortly after acceptance, before technical editing, formatting and proof reading. Using this free service, authors can make their results available to the community, in citable form, before we publish the edited article. We will replace this *Accepted Manuscript* with the edited and formatted *Advance Article* as soon as it is available.

You can find more information about *Accepted Manuscripts* in the Information for Authors.

Please note that technical editing may introduce minor changes to the text and/or graphics, which may alter content. The journal's standard Terms & Conditions and the Ethical guidelines still apply. In no event shall the Royal Society of Chemistry be held responsible for any errors or omissions in this *Accepted Manuscript* or any consequences arising from the use of any information it contains.

ROYAL SOCIETY OF CHEMISTRY

www.rsc.org/pccp

Physical Chemistry Chemical Physics
CREATED USING THE RSC LaTeX PCCP ARTICLE TEMPLATE – SEE www.rsc.org/electronicfiles FOR DETAILS
ARTICLE TYPE www. rsc.org/xxxxxx | XXXXXXXX

Influence of polaron formation to exciton dissociation

Guangqi Li,[a]

Received Xth XXXXXXXXXX 20XX, Accepted Xth XXXXXXXXX 20XX
First published on the web Xth XXXXXXXXXX 200X
DOI: 10.1039/b000000x

A linear tight-binding model was used to examine the yield of exciton dissociation under the influence of the electron-vibration interaction. The system consists of a linear chain, coupled to a single vibration, and electron-vibration interaction is permitted to occur on the certain sites. In the presence of this interaction, population tends to localize to build a polaron. System loses polaron trapping energy to the environment through its coupling to the bath environment, and loses population due to the injection to the electrode at the terminal site. A self-energy term was generated from the population injection, and was added to the energy level of the last site, working as a sink function to absorb the electron and measure the yield. This injection occurs only when the electron energy is inside and around the band. When the electron energy is outside the tight-binding band, population injection is inhibited. Our aim is to investigate the exciton dissociation effected by the competition between the the polaron formation and the population injection, via a process strongly influenced by the inter-site coupling and the electron-vibration interaction.

1 Introduction

Solar cell energy is promising as a major response to the challenge of green energy capture[1]. Because of low cost, mechanical flexibility and the versatility of organic materials designs[2–16], organic photovoltic cells (OPVC) offer the potential to change our energy landscape. The bulk heterojunction (BHJ) cell is the most common approach to OPVC; it consists of mixed donor (D) and acceptor (A) species that form interpenetrating connective networks[17–29]. Many of the theoretical analysis works on solar cells are based on the Marcus theory[30], where the initial and final states of the electron transfer process are fully equilibrated polarons, localized on different sites with the transitions between them being evaluated within the assumptions of transition state theory.

The exciton dissociation follows shortly after the initial photo-excitation (usually of the D species), involving a HOMO to LUMO transition of that molecule, which occurs during the interface between D and A[31–33]. Recent work[34] proposed that exciton dissociate can also occur away from the interface and generate separated electrons and holes. Due to the strong Coulomb attraction between electrons and holes, it is difficult for the electron to escape even after transfer to the interface, and the (charge-transfer) exciton remains bound to the interface until thermal release or recombination. At the interface, electron trapping and scattering drastically influence to the charge transport properties[35–44]. Accounting the electron-vibronic interaction is important for modeling these processes with higher accuracy, especially the bound polaron pair mechanism had been proposed as an intermediate to the carrier separation[45–47]. With this interaction, population localizes to build a polaron[48], inducing "self-trapping"at the local site[15,26,27,49–60]. A polaron is a charge (electron or hole), with the nuclear distortion of the charge's surroundings. Under the photo-excitation, polaron pairs may be generated in the BHJ and they can dissociate to form free charge carriers (electron and hole), which may decay back to the ground state through nonradiative recombination, or recombine bimolecularly back to polaron pair.

In the recent work[61], a one-dimensional tight-binding model is used to describe dissociative charge transfer in BHJ cell, where a "self energy"term is added to the edge site to probe the yield of the exciton dissociation. In another work[52,53], the electron-vibration interaction is introduced to form a polaron (charge localized state) and its influence on the electron transfer process is examined. In this paper, a tight-biding model is used to examine the influence of the electron-vibration interaction on exciton dissociation. The electron-vibration interaction occurs at the middle site of the chain. Vibrational energy exchange occurs between the system vibration and the phonon bath, and a quantum master equation was used to deal with this coupling via second-order perturbation theory. The "self energy"term retained working as a sink function to measure the yield of exciton dissociation. When the system energy is inside the band, population injection into the electrode occurs. The yield is not only effected by the electron-vibration interaction and inter-site coupling, but also depends upon the so-called LUMO-LUMO gap (the energy difference between sites 0 and 1 in our model). The coulomb interaction between the moving electron and the hole left behind is not accounting, and the issue addressed herein is that how the polaron formation effects the yield of the exciton dis-

[a]*Department of Chemistry, Northwestern University, Evanston IL, 60208, USA*

Physical Chemistry Chemical Physics Accepted Manuscript

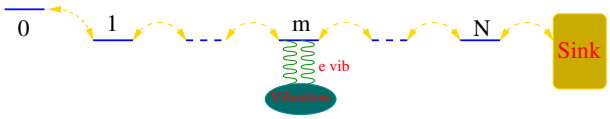

Fig. 1 The scheme of a linear chain including N+1 site. The electron-vibration coupling occurs on the middle site m. The sink represented the effect of the rest semi-infinite chain beyond site N.

sociation, by competing with the sink absorption. The yield of such a processes is determined by three parameter: the electron-vibration interaction, the inter-site coupling and the initial injection energy. We start by formulating the basic Hamiltonian model and theoretical methods (including "self energy", quantum master equation and the yield calculation) in Section II. Numerical calculation and discussions of the influence from the electron-vibration interaction, inter-site coupling and the initial injection energy to the yield is examined in section III. Section IV concludes.

2 Theoretical model

The Hamiltonian of the system shown in Fig.1 (interacting with a vibrational bath) is

$$H = H_S + H_B + H_{SB} \,, \tag{1}$$

$$H_S = \sum_{l=0}^{N} \varepsilon_l c_l^\dagger c_l + \mathrm{V} \sum_{l=0}^{N-1} (c_l^\dagger c_{l+1} + c_{l+1}^\dagger c_l) + \hbar\omega_0 d_0^\dagger d_0 + \alpha_0 c_m^\dagger c_m (d_0^\dagger + d_0) \,, \tag{2}$$

$$H_B = \sum_{s=1}^{\infty} \hbar\omega_s d_s^\dagger d_s \,, \tag{3}$$

$$H_{SB} = \sum_{s=1}^{\infty} \lambda_s (d_0^\dagger d_s + d_s^\dagger d_0) \,, \tag{4}$$

here H_S is the linear system Hamiltonian which includes N+1 sites and is coupled to a single vibration, H_B is the bath environment (secondary phonon) and H_{SB} is the coupling between the system vibration and the environment. In H_S, operator $c_l^\dagger$ (c_l) creates (annihilates) an electron in site l, ε_l is the on-site energy of site l, V is the coupling between the two nearest neighbor sites. The third term in right of Eq. 2 is the system vibration with the frequency ω_0, $d_0^\dagger$ (d_0) creates (annihilate) an vibrionic state, and the last term indicts the interaction (occurring on site m) between the electronic states and the vibration, with the coupling parameter α_0. The secondary vibration (H_B) couples to the primary vibration with coupling strength λ_s, as shown in Eq. 4 (using the rotating wave approximation). $d_s^\dagger$ (d_s) create (annihilate) one vibration with the frequency ω_s.

2.1 Self energy

Our full system includes a semi-infinite chain. Here a finite system is used and the effect of the rest is taken into account by adjusting the energy of site N by a self energy term[62–65]

$$\Sigma(E) = \frac{E \pm \sqrt{E^2 - 4\mathrm{V}^2}}{2} \,, \tag{5}$$

Here E is the injection energy. When E is in the energy band, i.e., $-2\mathrm{V} \le E \le 2\mathrm{V}$, $\Sigma(E)$ is a complex number as

$$\Sigma(E) = \frac{E - i\sqrt{4\mathrm{V}^2 - E^2}}{2} = \Lambda(E) - \frac{i}{2}\Gamma(E) \,, \tag{6}$$

with $\Lambda(E) = \frac{E}{2}$ and $\Gamma(E) = \sqrt{4\mathrm{V}^2 - E^2}$ being real numbers. When E is outside the energy band, i.e., $E \le -2\mathrm{V}$ or $E \ge 2\mathrm{V}$, $\Sigma(E)$ is a real number as

$$\Sigma(E) = \frac{E + \sqrt{E^2 - 4\mathrm{V}^2}}{2} \,, \quad for\ E \le -2\mathrm{V} \,, \tag{7}$$

$$\Sigma(E) = \frac{E - \sqrt{E^2 - 4\mathrm{V}^2}}{2} \,, \quad for\ E \ge 2\mathrm{V} \,. \tag{8}$$

In Eqs. 7 and 8, $+$ and $-$ are selected respectively because $\Sigma(E) \to 0$ when $E \to \infty$. We take this term as an additional energy at site N, acting as a sink that absorbs the outgoing particle. The Hamiltonian H_{sink} of this part can be expressed as

$$H_{sink}(t) = \sum_{\nu} \Sigma(E) |\mathrm{N}, \nu><\mathrm{N}, \nu| = \sum_{\nu} (\Lambda(E) - \frac{i}{2}\Gamma(E)) |\mathrm{N}, \nu><\mathrm{N}, \nu| \,. \tag{9}$$

which is a sum at site N over the different vibrational levels ν. $E = \bar{E}_S(t) - \hbar\omega_0\nu$ is the injected energy for the electron scattering from the excited vibrational level ν. $\bar{E}_S(t)$ is the time-dependent (renormalized) system energy which can be obtained from Eq. 15.

2.2 Quantum master equation

The density matrix ρ_T of the whole system can be written as $\rho_T = \mathrm{Tr}_B\{\rho_T\} \otimes \rho_B$. Using this definition, the reduced density matrix ρ_S of the molecular wire can be expressed as $\rho_S = \mathrm{Tr}_B\{\rho_T\}$ and the new relationship $\rho_T = \rho_S \otimes \rho_B$ is obtained. The density matrices ρ_S and ρ_B relate to H_S and H_B respectively. We assume that ρ_B is in initially in its equilibrium state. The trace operators Tr_S and Tr_B relate to the Hamiltonians H_S and H_B respectively. Then the quantum master equation (QME) for the calculation of ρ_S is[66,67]

$$i\hbar \frac{\partial \rho_S(t)}{\partial t} = [H_S + H_{sink}(t), \rho_S(t)] - i\hbar\gamma_0/2[d_0^\dagger d_0 \rho_S(t) + \rho_S(t) d_0^\dagger d_0 - 2 d_0 \rho_S(t) d_0^\dagger] \,, \tag{10}$$

Physical Chemistry Chemical Physics Accepted Manuscript

This journal is © The Royal Society of Chemistry [year]

γ_0 is the phonon relaxation rate induced by the active phonon/bath coupling, which is obtained from the imaginary part of the active phonon self energy Σ as

$$\gamma_0(\omega)/2 = \frac{1}{\hbar}\mathrm{Im}\{\Sigma_{\mathrm{phonon}}(\omega)\} = \frac{1}{\hbar}\sum_{\mathrm{s}}|\lambda_{\mathrm{s}}|^2\delta(\hbar\omega - \hbar\omega_{\mathrm{s}}) \ . \tag{11}$$

The time-dependent evolution of the system density matrix ρ_S is treated essentially exactly[68], using the basis set $\{|\mathrm{n},\nu>\}$. Here n and ν denote the electronic state localized on site n and the vibrational state ν of the primary oscillator. In the numerical calculation we truncate the set $\{\nu\}$ at some value, ν_{max} and test for convergence as ν_{max} increases. Eq. 10 can be rewritten as

$$\begin{aligned} i\hbar\frac{\partial\rho_{n\nu,n'\nu'}(t)}{\partial t} &= [H_S + H_{sink}(t), \rho_S(t)]_{n\nu,n'\nu'} \\ &- i\hbar\gamma_0(\nu+\nu')\rho_{n\nu,n'\nu'}\delta_{n,n'}/2 \\ &+ i\hbar\gamma_0\sqrt{\nu+1}\sqrt{\nu'+1}\rho_{n,\nu+1,n',\nu'+1} \ , \end{aligned} \tag{12}$$

where the first term in the right side of Eq. 12 comes from the contribution of primary system Hamiltonian $H_S + H_{sink}(t)$. The second part comes from the first two terms in the bracket on the right side of Eq. 10 and the last term involves energy transfer from the higher to the lower vibrational levels. Because of the zero temperature and Bose-Einstein distribution function $N_B(\omega) = \dfrac{1}{e^{\hbar\omega/KT}-1} \equiv 0$ (except for the ground vibrational level), the energy transfer only happens from the higher levels to its nearest lower level. In the non-zero temperature, the Bose-Einstein distribution function is not zero, some terms represent the transfer from lower vibrational levels to higher vibrational levels showing up in Eq. 10[67].

2.3 Yield of the exciton dissociation and the on-site population

The yield of the exciton dissociation is measured by the Hamiltonian H_{sink} in Eq. 9, and it is expressed as

$$\begin{aligned} \mathrm{Y} &= i\sum_{\nu}\int_0^{\infty} dt\mathrm{Tr}\{H_{sink}\rho - \rho H_{sink}^{+}\} \\ &= \sum_{\nu}\int_0^{\infty} dt\sum_{\nu}\rho_{\mathrm{N}\nu,\mathrm{N}\nu}\Gamma(\bar{E}_S(t) - \nu\hbar\omega_0) \ . \end{aligned} \tag{13}$$

Here $\rho_{\mathrm{N}\nu,\mathrm{N}\nu}$ is the population on the νth vibrational level on site N. Γ is the imaginary part of self energy Σ (in Eq. 6) and is the transfer rate between the system and the injection electrode. When $\bar{E}_S(t) - \nu\hbar\omega_0$ is inside the band, Γ is non-zero number and the population will be absorbed. When $\bar{E}_S(t) - \nu\hbar\omega_0$ is outside the band, Γ is zero, and the population absorption is stopped. The population injection and sink absorption are dependent on the time-dependent renormalized system energy $\bar{E}_S(t)$. Due to the coupling of the system vibration to the bath environment, the system loses its energy through energy exchange with the bath environment. The real time-dependent system energy $E_S(t)$ is

$$E_S(t) = \mathrm{Tr}\{H_S \bullet \rho_S(t)\} \ , \tag{14}$$

and a renormalized system energy $\bar{E}_S(t)$ is

$$\bar{E}_S(t) = E_S(t)/\mathrm{Tr}\{\rho_S(t)\} = \mathrm{Tr}\{H_S \bullet \rho_S(t)\}/\mathrm{Tr}\{\rho_S(t)\} \ . \tag{15}$$

Both $E_S(t)$, $\bar{E}_S(t)$ and $\mathrm{Tr}\{\rho_S(t)\}$ will continue to decrease until the system reaches its steady state. The population on site 8 (the polaron population) at any time t is

$$P_8(t) = \mathrm{Tr}\{c_8^{\dagger}(t)c_8(t)\rho_S(t)\} \ . \tag{16}$$

3 polaron formation and exciton dissociation

For the numerical simulation N=15; the maximum vibrational number $\nu_{max} = 9$; $\omega_0 = 0.1eV$; $\gamma_0 = 0.04eV$; $\varepsilon_8 = -0.16eV$ and $\varepsilon_l = 0$ for the other sites are set. In the following, the processes of polaron formation, system relaxation and excitation yield are examined by varying the electron-vibration interaction α_0, the tunneling parameter V, and the LUMO-LUMO energy gap ε_0 ($\varepsilon_1 = 0$). The electron-vibration interaction occurs on site 8 (m=8), and the variation of ε_8 will be examined.

In the numerical simulation, it is better to account a system including more sites. Due to the calculation difficulty of dealing with the large density matrix, N=15 is taken. Here site energy ε_8 which is lower than its nearest neighbor, represents the trapping energy to form a polaron in this site. The inter-site coupling parameter V is key role for the polaron formation process. In order to form a polaron, the energy gap (ε_8) should be in the same order with V. If this gap is too large than V, charge transfer will stop. If this gap is too small, polaron will not build here. Here V varies from 0.05eV-0.15eV, which is similar to that had been used to investigate the charge transfer processes in organic photovoltaic cells[69].

ω_0 = 0.1 eV is selected according to V. When ω_0 is smaller than V, the system vibration becomes slower. With a large ω_0, vibrations becomes faster. γ_0 is relative to the relax processes. With a large γ_0, the relax processes become faster. With a small γ_0, system will take long time to reach the steady state.

3.1 $\nu_{\max}$ and the site energy ε_8

In this section, we examine two parameters: the vibrational maximum number ν_{max} and the site energy ε_8. In absence of the sink function, population injection into the electrode is stopped. The total population of the system remains 1 with

Physical Chemistry Chemical Physics Accepted Manuscript

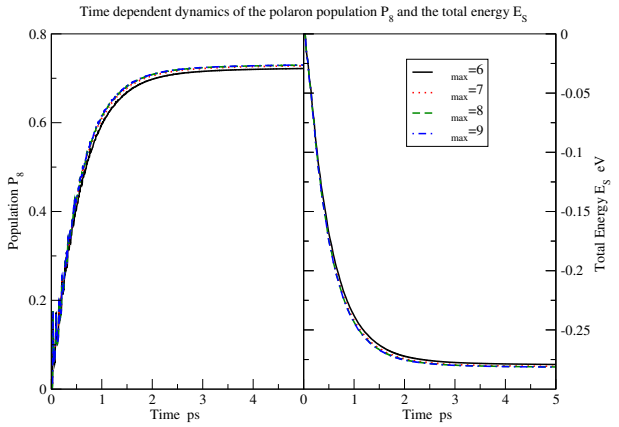

Fig. 2 Time-dependent polaron population P_8 and the total energy E_S are shown with different vibrational number $\nu_{\max}$. $\varepsilon_8 = -0.16eV$ and $\varepsilon_l = 0$ for the rest sites. $V = \alpha = 0.1eV$. The sink absorbing function is off ($H_{sink} = 0$ in Eq. 9).

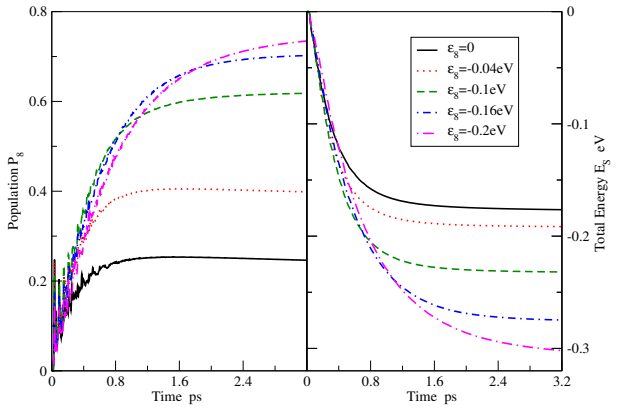

Fig. 3 Time-dependent polaron population P_8 and the total energy E_S are shown with different site energy ε_8. $\varepsilon_l = 0$ for the rest sites. $V = \alpha_0 = 0.1eV$. The sink absorbing function is off ($H_{sink} = 0$ is used in Eq. 9).

$\bar{E}_S = E_S$. Due to the coupling to the bath environment, E_S keeps decreasing until the system reaches its steady state.

In Fig. 2, polaron population P_8 and total energy E_S are examined via changing the maximum vibrational number $\nu_{\max}$. Due to the electron-vibration interaction, population tends to localize to form a polaron on site 8, and the system energy E_S keeps decreasing until the system reaches its steady state. When $\nu_{\max}$ is as larger than 7, 8 or 9, the time dependent processes are convergent. $\nu_{\max} = 9$ will be used in the following calculation.

Fig. 3 show the changing of P_8 and E_S as a function of time with different ε_8. With a lower site energy ε_8, more population will be localized on this site to form a polaron, with the system energy E_S also relaxing to a much lower value. With ε_8 dropping, more population will be localized on site 8. However with a much lower ε_8, population transfer from the nearest sites to site 8 is inhibited due to the larger energy gap between site 8 and its neighbor sites. In the following calculations, $\varepsilon_8 = -0.16eV$ and $\varepsilon_l = 0$ for the rest sites will be used.

3.2 influence of the inter-site coupling V

The tunneling parameter V fixes the width of the band (4V)*, and influences the polaron formation, and population injection. With a smaller V (narrow band), population tends to localize to form a polaron[48,52,53] (the polaron model of Holstein[48] is based on the narrow band). With increasing V, polaron population P_8 decreases as shown in Fig. 4. Especially when V is large enough, poplaron will not be formed[52,53], and tunneling mechanism will dominate the charge transfer rather than hopping mechanism[52]. Population P_8 with sink absorption is smaller than that without the sink function, because of the population injection. Due to the energy exchange with the bath environment, the renormalized energy $\bar{E}_S$ decreases with time (shown in Fig. 5). When $\bar{E}_S$ is outside the band (lower than $-2V$), population injection is stopped. Part of the population can survive in the chain, reaching steady state together with the system.

Yields of the exciton dissociation are show in the left panel of Fig. 5. Yield increases with increasing V since the large V will prevent the population to form polaron. With smaller V, more population tends to localize on site 8 to form a polaron.

3.3 influence from the electron-vibration interaction

As shown in Fig. 6, in the presence of the electron-vibration interaction, population tends to localize to build a polaron. With increasing α_0, more population is localized on site 8, which will prevent the population absorption. Yield decreases; system loses more energy to the environment; both E_S and its normalized value $\bar{E}_S$ will relax to a much lower value.

With a smaller tunneling parameter V or with a large electron-vibration coupling α_0, more population tend to localize to form a polaron, rather than to be absorbed by the sink. More population can survive in the chain, and the system energy E_S can reach a much lower value. While with a larger V or a smaller α_0, more population will be injected and absorbed.

To form a polaron, the energy gap (ε_8) and the inter-site tunneling parameter V are the key role. If V is large, tunneling mechanism dominates the transfer processes, polaron will not be formed, even with increasing α_0. This had been examined in our previous paper[52]. Polaron will always be formed if the

* here the band is relative to system with the Hamiltonian H_S. The Hamiltonian of the sink is not accounting

Physical Chemistry Chemical Physics Accepted Manuscript

This journal is © The Royal Society of Chemistry [year]

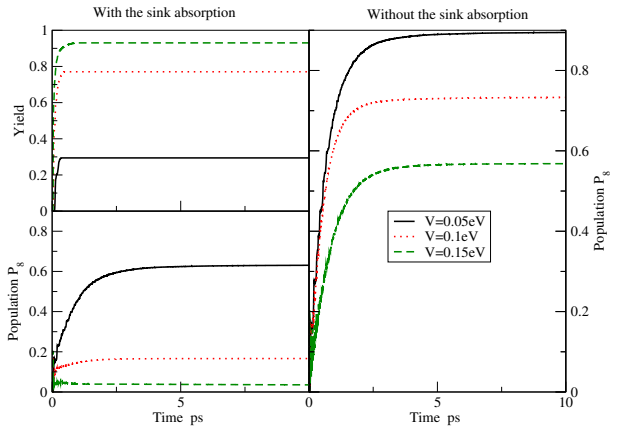

Fig. 4 Yield (left panel) and polaron population P_8 are shown with different inter-site coupling parameter V. $\alpha_0 = 0.1eV$. The sink absorbing function is on (left panel) and off (right panel). Yield=0 in the case without the sink absorption. $\varepsilon_8 = -0.16eV$ and $\varepsilon_l = 0$ for the rest sites.

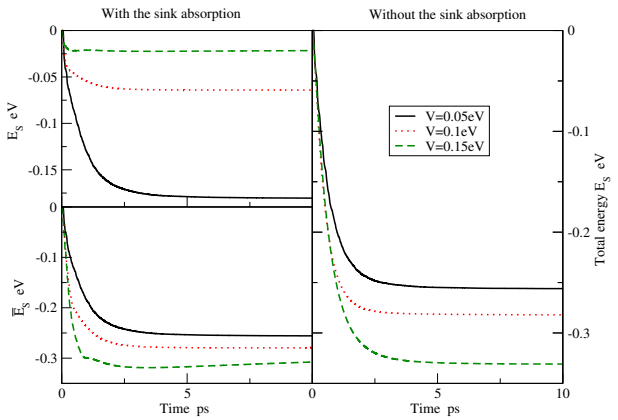

Fig. 5 Real system energy E_S and the renormalized energy $\bar{E}_S$ (left panel) are shown with different inter-site coupling parameter V. $\bar{E}_S = E_S$ in the case without the sink absorption. Same parameters are used as to Fig. 4.

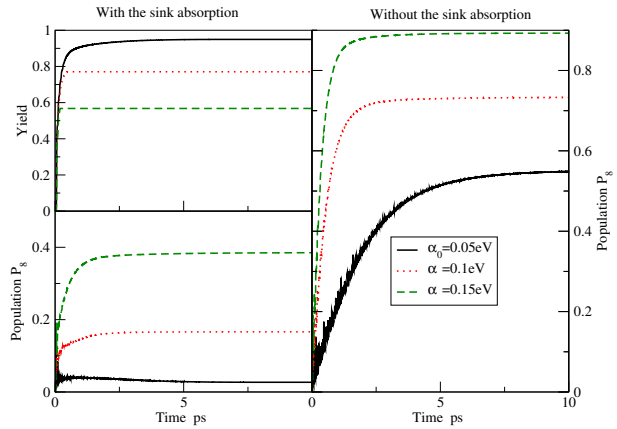

Fig. 6 Yield (left panel) and the polaron population P_8 are shown with different electron-vibration interaction parameter α_0. $V = 0.1eV$. The sink absorbing function is on (left panel) and off (right panel). Yield=0 in the case without sink absorption. $\varepsilon_8 = -0.16eV$ and $\varepsilon_l = 0$ for the rest sites.

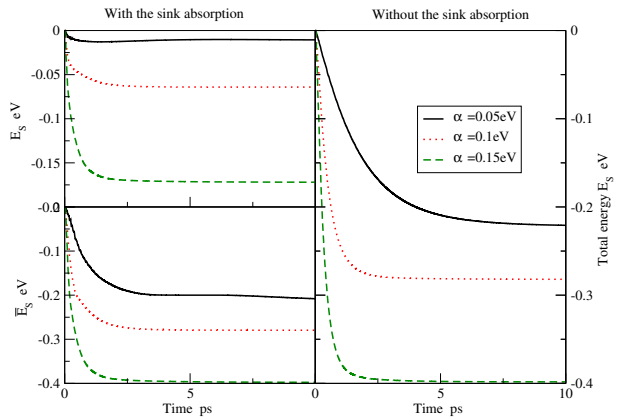

Fig. 7 Real system energy E_S and the renormalized energy $\bar{E}_S$ (left panel) are shown with different electron-vibration interaction parameter α_0. $\bar{E}_S = E_S$ in the case without the sink absorption. Same parameters are used as to Fig. 6.

Physical Chemistry Chemical Physics Accepted Manuscript

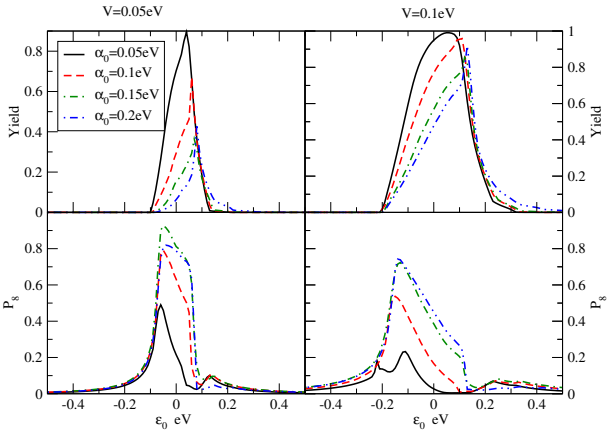

Fig. 8 Yield and population P_8 are shown as a function of the injection energy ε_0 with different electron-vibration coupling parameter α_0, and in the presence of the sink absorption. V=0.05eV (left panel) and V=0.1eV (right panel). $\varepsilon_8 = -0.16eV$ and $\varepsilon_l = 0$ for the rest sites.

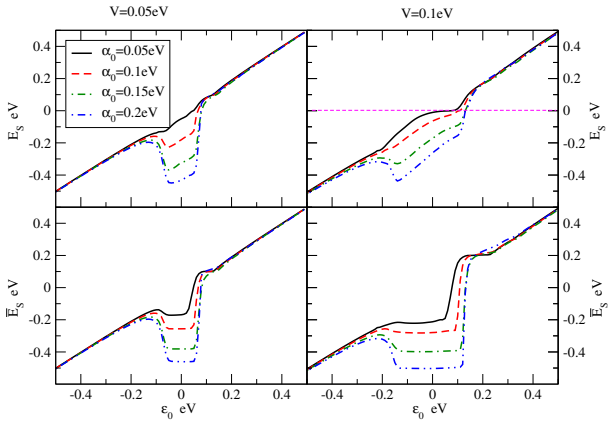

Fig. 9 System energy E_S and the renormalized energy $\bar{E}_S$ are shown as as a function of the injection energy ε_0 with different electron-vibration coupling parameter α_0, and in the presence of the sink absorption. V=0.05eV (left panel) and V=0.1eV (right panel). Some values of E_S are near zero (red thin dashed line), because most population are absorbed due to large V. $\varepsilon_8 = -0.16eV$ and $\varepsilon_l = 0$ for the rest sites.

V matches the energy gap (ε_8). Thus there is no critical V value that no polaron would be formed.

3.4 injection energy ε_0

In this section, the yield of exciton dissociation, the localized population on site 8 (polaron population), the system energy E_S and its normalized value $\bar{E}_S$, are examined via varying the injection energy ε_0, as shown in Figs. 8 and 9. When ε_0 is near or inside the band ($\sim 4V$), population transfer from site 0 to its neighbor sites occurs. A polaron is formed (for small enough V) to prevent the population injection. System energy E_S keeps decreasing (even tends to be zero when all population are injected), due to the energy exchange with the bath environment. Yield of the exciton dissociation keeps increasing and reaches its peak values, when ε_0 is around zero. Population P_8 also increases and reaches a peak value.

When ε_0 is outside the band ($\sim 4V$), due to the large energy gap between sites 0 and its neighbor sites, the population transfer from site 0 to its next is inhibited. As a results, population is localized on site 0, with yield=0 and system energy $E_S = \varepsilon_0$, showing linear behavior (Fig. 9). When ε_0 is inside the band, system loses its energy to the environment and E_S keeps decreasing. When the system energy E_S is outside the band, population injection is stopped, and the yield remains constant.

4 conclusion

In this paper we are interested in situations where electronic band motion, population injection competes with polaron formation. These considerations are relevant to recently studied models of photovoltaic cells[61,70], where electrons (or holes) are injected at some location in the system. The yield of such processes, determined by the competition between electronic motion and loss processes[61] (e.g. carrier recombination) is expected to be sensitive to electron-phonon interactions, and in particular to transient polaron formation.

Deeply understanding the exciton dissociation is a challenge, and herein a plethora of models has been applied to the understanding of the transport and the overall functioning of these devices. Here a tight-binding model is used to examine the effects of acceptor bandwidth, injection energy gaps, charge trapping. The effect from the coulomb binding and disorder in the acceptor band are not accounted here. The model assumes one-dimensional tight-binding electronic behavior with an electron-vibration interaction being permitted to occur on the certain site. In the present of this interaction, population tends to localize to build a polaron. Due to the coupling between the system vibration and the bath environment (bath phonon), the system loses its energy. A "self-energy"term generated from the population injection into the electrode, is added to the energy level of the last site, working as a sink function to absorb the population and measure the yield of the exciton dissociation. This term is assumed to be a function of the (renormalized) system energy. When this renormalized system energy is inside and near the band (from -2V to 2V), the population is injected into the electrode and is absorbed. When the system energy is outside the band, the injection does not take place. The system energy is strongly influenced by the the inter-site coupling parame-

Physical Chemistry Chemical Physics Accepted Manuscript

This journal is © The Royal Society of Chemistry [year]

ter V, the electron-vibration interaction parameter α_0. With a smaller V and a larger α_0, population tends to be localized to form a polaron, which prevents the population absorption and reduces the yield of the exciton dissociation.

The exoergicity ε_0 of the charge separation $D^*A \rightarrow D^+A^-$, usually referred to as the LUMO-LUMO gap, provides enough energy for the charge separation process to overcome the D^+A^- coulomb attraction. When ε_0 is around and inside the band, population transfer from site 0 to its neighbor next occurs, the vibrational levels can be populated and the system begin to lose its energy. When the population is injected into the electrode, absorption occurs only if the system energy $\bar{E}_S$ is near and inside the band. When $\bar{E}_S$ is outside the band, no injection occurs, and the left population on the chain can survive. Later both E_S and $\bar{E}_S$ keep decreasing until the system reaches its steady state. However, when the injection energy ε_0 is too far away from the band, population transfer from site 0 to site 1 is inhibited due to the large energy gap between sites 0 and 1. No transfer occurs and no energy loses. To generate free charge carriers, the electron-hole pair needs to overcome the coulomb interaction, which is induced between the moving electron and the hole. However the free charge carriers may recombine bimolecularly back to form a polaron pair. Exciton recombination is a completely relaxation process that reduces the probability of charge separation. In this paper, only a single vibration is accounted, together with the electron-vibration interaction permitted to occur on certain site. Our aim is to examine the exciton dissociation effected by the competition between the the polaron formation and the population injection. In the real system, more vibration modes can occur on one single site, for example in the biology system (photosynthesis I)[71], and examining the polaron formation with quantum method becomes difficulty. The influence from the coulomb interaction, the recombination, and more electron-vibration interactions will be examine in our future work. The model and the system Hamiltonian can be used to examine the transfer processes for both the hole and the electron.

Acknowledgement The author would like to thank the useful discuss with Aharham Nitzan, Mark Ratner and Bijan Movaghar. The author would also like to acknowledge an anonymous referee whose remarks significantly helped to improve the presentation of results. This work was supported by the Non-Equilibrium Energy Research Center (NERC) which is an Energy Frontier Research Center funded by the U.S. Department of Energy, Office of Science, Office of Basic Energy Sciences under Award Number DE-SC0000989.

References

1 N. S. Lewis, *Science*, 2007, **315**, 798.
2 J. D. Servaites, M. A. Ratner and T. J. Marks, *Appl. Phys. Lett.*, 2009, **95**, 163302.
3 B. Kippelen and J. L. Brédas, *Energy Environ. Sci.*, 2009, **2**, 251.
4 S. Gunes, H. Neugebauer and N. S. Sariciftci, *Chem. Rev.*, 2007, **107**, 1324.
5 J. D. Servaites, S. Yeganeh, M. A. Ratner and T. J. Marks, *Adv. Func. Mat.*, 2010, **20**, 97.
6 C. W. Tang, *Appl. Phys. Lett.*, 1986, **48**, 183.
7 K. M. Coakley and M. D. McGehee, *Chem. Mater.*, 2004, **16**, 4533.
8 G. Dennler, M. C. Scharber and C. J. Brabec, *Adv. Mater.*, 2009, **21**, 1.
9 J. L. Brédas, J. Cornil and A. J. Heeger, *Adv. Mater.*, 1996, **8**, 447.
10 T. M. Clarke and J. R. Durrant, *Chem. Rev.*, 2010, **110**, 6736.
11 B. C. Thompson and J. M. J. Fréchet, *Angew. Chem. Int. Ed.*, 2008, **47**, 58.
12 J. Lee, K. Vandewal, S. R. Yost, M. E. Bahlke, L. Goris, M. A. Baldo, J. V. Manca and T. V. Voorhis, *J. Am. Chem. Soc.*, 2010, **132**, 11878.
13 D. Veldman, O. Lpek, S. C. J. Meskers, J. Sweelssen, M. M. Koetse, S. C. Veenstra, J. M. Kroon, S. S. van Bavel, J. Loos and R. A. J. Janssen, *J. Am. Chem. Soc.*, 2008, **130**, 7721.
14 I.-W. Hwang, D. Moses and A. J. Heeger, *J. Phys. Chem. C*, 2008, **112**, 4350.
15 H. j. Cha, H.-N. Kim, T.-K. An, M.-S. Kang, S.-K. Kwon, Y.-H. Kim and C.-E. Park, *Appl. Mater. Interfaces*, 2014, **6**, 15774.
16 S. R. Yost, E. Hontz, D. P. McMahon and T. V. Voorhis, *Top Curr Chem*, 2014, **352**, 103.
17 Y. Liang, D. Feng, Y. Wu, S.-T. Tsai, G. Li, C. Ray and L. Yu, *J. Am. Chem. Soc.*, 2009, **131**, 7792.
18 S. H. Park, A. Roy, S. Beaupr, S. Cho, N. Coates, J. S. Moon, D. Moses, M. Leclerc, K. Lee and A. J. Heeger, *Nat. Photonics*, 2009, **3**, 297.
19 J. Peet, J. Y. Kim, N. E. Coates, W. L. Ma, D. Moses, A. J. Heeger and G. C. Bazan, *Nature Mater*, 2007, **6**, 497.
20 R. B. Ross, C. M. Cardona, D. M. Guldi, S. G. Sankaranarayanan, M. O. Reese, N. Kopidakis, J. Peet, B. Walker, G. C. Bazan, E. V. Keuren, B. C. Holloway and M. Drees, *Nature Mater*, 2009, **8**, 208.
21 R. Kroon, M. Lenes, J. C. Hummelen, P. W. M. Blom and B. D. Boer, *Polym. Rev.*, 2008, **48**, 531.
22 L. X. Chen, S. Q. Xiao and L. P. Yu, *J. Phys. Chem. B*, 2006, **110**, 11730.
23 J. C. Guo, Y. Y. Liang, S. Q. Xiao, J. Szarko, M. Sprung, M. K. Mukhopadhyay, J. Wang, L. P. Yu, and L. X. Chen,

Physical Chemistry Chemical Physics Accepted Manuscript

New J. Chem., 2009, **33**, 1497.
24 A. Datta and S. K. Pati, *Chemical Society Reviews*, 2006, **35**, 1305–1323.
25 A. Datta, F. Terenziani and A. Painelli, *ChemPhysChem*, 2006, **7**, 2168–2174.
26 S. Bera, N. Gheeraert, S. Fratini, S. Ciuchi and S. Florens, *Phys. Rev. B*, 2015, **91**, 041107(R).
27 S. Latini, E. Perfetto, A.-M. Uimonen, R. van Leeuwen and G. Stefanucci, *Phys. Rev. B*, 2014, **89**, 075306.
28 M. Olguin, R. R. Zope and T. Baruah, *J. Chem. Phys.*, 2013, **138**, 074306.
29 J. Ye, K.-W. Sun, Y. Zhao, Y. Yu, C. Lee and J.-S. Cao, *J. Chem. Phys.*, 2012, **136**, 245104.
30 R. A. Marcus, *J. Chem. Phys.*, 1956, **24**, 966.
31 X. Y. Zhu, Q. Yang and M. Muntwiler, *Acc. Chem. Res.*, 2009, **42**, 1779.
32 M. Scharber, D. Muhlbacher, M. Koppe, P. Denk, C. Waldauf, A. J. Heeger and C. J. Brabec, *Adv. Mater.*, 2006, **18**, 789.
33 B. P. Rand, D. P. Burk and S. R. Forrest, *Phys. Rev. B*, 2007, **75**, 115327.
34 D. Caruso and A. Troisi, *PNAS*, 2012, **109**, 13498.
35 A. Nitzan, *Ann. Rev. Phys. Chem.*, 2001, **52**, 681–750.
36 A. Nitzan, *Adv. Chem. Phys.*, 2014, **157**, 135.
37 A. Nitzan, *Chemical Dynamics in condensed Phases*, Oxford, Oxford, 2006.
38 D. Golež, J. Bonča, L. Vidmar and S. A. Trugman, *Phys. Rev. Lett.*, 2012, **109**, 236402.
39 E. R. Bittner, S. Karabunarliev and A. Ye, *J. Chem. Phys.*, 2005, **122**, 034707.
40 S.-J. Xu, G.-Q. Li, S.-J. Xiong, S.-Y. Tong, C.-M. Che, W. Liu and M.-F. Li, *J. Chem. Phys.*, 2005, **122**, 244712.
41 S.-J. Xu, G.-Q. Li, Y.-J. Wang, Y. Zhao, G.-H. Chen, D.-G. Zhao, J.-J. Zhu, H. Yang, D.-P. Yu and J.-N. Wang, *Appl. Phys. Lett.*, 2006, **88**, 083123.
42 Y. Zhao, G.-Q. Li, J. Sun and W.-H. Wang, *J. Chem. Phys.*, 2008, **129**, 124114.
43 Y. Zhao, B. Luo, Y.-Y. Zhang and J. Ye, *J. Chem. Phys.*, 2012, **137**, 084113.
44 B. Popescu, P. B. Woiczikowski, M. Elstner and U. Kleinekathfer, *Phys. Rev. Lett.*, 2012, **109**, 176802.
45 W.-S. Koh, M. Pant, Y. A. Akimov, W.-P. Goh and Y.-N. Li, *IEEE J. Photovoltaics*, 2011, **1**, 2156.
46 S. Shoaee, S. Subramaniyan, H. Xin, C. Keiderling, P. S. Tuladhar, F. Jamieson, S. A. Jenekhe and J. R. Durrant, *adv. Funct. Mater. DOI: 10.1002/adfm.201203148*, 2013, **23**, 3286.
47 N. C. Giebink, B. E. Lassiter, G. P. Wiederrecht, M. R. Wasielewski and S. R. Forrest, *Phys. Rev. B*, 2010, **82**, 155306.
48 T. Holstein, *Ann. Phys.*, 1959, **8**, 325–342.
49 M. Galperin, M. A. Ratner and A. Nitzan, *Nano Letter*, 2005, **5**, 125–130.
50 M. Galperin, M. A. Ratner, A. Nitzan and A. Troisi, *Science*, 2008, **319**, 1056–1060.
51 G.-Q. Li, B. Movaghar and M. A. Ratner, *J. Phys. Chem. C*, 2013, **117**, 850–857.
52 G.-Q. Li, B. Movaghar, A. Nitzan and M. A. Ratner, *J. Chem. Phys.*, 2013, **138**, 044112.
53 G.-Q. Li, B. Movaghar and M. A. Ratner, *Phys. Rev. B*, 2013, **87**, 094302.
54 S.-J. Xu, G.-Q. Li, S.-J. Xiong and C.-M. Che, *J. Appl. Phys.*, 2006, **99**, 073508.
55 S.-L. Shi, G.-Q. Li, , S.-J. Xu, Y. Zhao and G.-H. Chen, *J. Phys. Chem. B*, 2006, **110**, 10475.
56 M. G. Velarde, A.P.Chetverikov, W. Ebeling, E. G. Wilson and K. J. Donovan, *Europhys. Lett.*, 2014, **106**, 27004.
57 M.-X. Cheng, G.-Q. Li, F. G. Thomas and X. Sun, *Commun. Theor. Phys.*, 2005, **43**, 1137.
58 X. Sun, G.-Q. Li and S. Li, *Current Applied Physics*, 2001, **1**, 371.
59 G.-Q. Li, X. Sun and S. Li, *Chinese Journal of Polymer Science*, 2001, **19**, 573.
60 X. Sun, R.-L. Fu, K. Yonemitsu and K. Nasu, *Phys. Rev. Lett.*, 2000, **84**, 2830.
61 G.-Q. Li, A. Nitzan and M. A. Ratner, *Phys. Chem. Chem. Phys.*, 2012, **14**, 14270–14276.
62 G. C. Solomon, D. Q. Andrews, R. P. V. Duyne and M. A. Ratner, *Phys. Chem. Chem. Phys.*, 2009, **10**, 257.
63 M. G. Reuter, T. Hansen, T. Seideman and M. A. Ratner, *J. Phys. Chem. A*, 2009, **113**, 4665–76.
64 D. Rai, O. Hod and A. Nitzan, *J. Phys. Chem. C*, 2010, **114**, 20583.
65 V. Ben-Moshe, D. Rai, S. S. Skourtis and A. Nitzan, *J. Chem. Phys.*, 2010, **133**, 054105.
66 S. Welack, M. Schreiber and U. Kleinekathöfer, *J. Chem. Phys.*, 2006, **124**, 044712–1–9.
67 U. Kleinekathöfer, G.-Q. Li, S. Welack and M. Schreiber, *Europhys. Lett.*, 2006, **75**, 139–145.
68 J. Bonča and S. A. Trugman, *Phys. Rev. Lett.*, 1995, **75**, 2566.
69 S. Gelinas, A. Rao, A. Kumar, S. L. Smith, A. W. Chin, J. Clark, T. S. van der Poll, G. C. Bazan and R. H. Friend, *Science*, 2014, **343**, 512.
70 M. Einax, M. Dierl and A. Nitzan, *J. Phys. Chem. C*, 2011, **115**, 21396.
71 V. D. Lakhno, *J. Bio. Phys.*, 2005, **31**, 145–159.

Physical Chemistry Chemical Physics Accepted Manuscript

This journal is © The Royal Society of Chemistry [year]